

*Communication*

## Three Cavity Tunable MEMS Fabry Perot Interferometer

**Avinash Parashar \***, Ankur Shah, Muthukumaran Packirisamy and Narayanswamy Sivakumar

Department of Mechanical and Industrial Engineering, EV 13-310, Concordia University,  
1515, St. Catherine West, Montreal, Quebec, Canada H3G 2W1

\*Author to whom correspondence should be addressed; E-mail: parasharavinash@yahoo.com

*Received: 25 October 2007 / Accepted: 29 November 2007 / Published: 4 December 2007*

---

**Abstract:** In this paper a four-mirror tunable micro electro-mechanical systems (MEMS) Fabry Perot Interferometer (FPI) concept is proposed with the mathematical model. The spectral range of the proposed FPI lies in the infrared spectrum ranging from 2400 to 4018 (nm). FPI can be finely tuned by deflecting the two middle mirrors (or by changing the three cavity lengths). Two different cases were separately considered for the tuning. In case one, tuning was achieved by deflecting mirror 2 only and in case two, both mirrors 2 and 3 were deflected for the tuning of the FPI.

**Keywords:** Fabry Perot Interferometer, IR Spectroscopy, Full width Half Maximum, MEMS

---

### 1. Introduction

Optical filters based on micro electro-mechanical systems (MEMS) are an enabling technology for hyper spectral images [1], [2] and micro spectrometer [3-5]. Infrared (IR) filters are high pass filters that block the visible light and pass IR light. They are characterized by their bandwidth at which maximum transmission is 50%.

MEMS based FPI usually consist of a vertically integrated structure composed of two mirrors separated by an air gap, wavelength tuning is achieved by applying the voltage between the two mirrors resulting in an electrostatic force which pulls the mirror closer. Main disadvantage associated with two mirrors FPI is limited spectral range with high bandwidth [6-9]. One development is in the area of tandem or multipass FPIs [10-12] in which a number of two mirror FPIs of different lengths are placed in series in order to realize a broad spectral range and a high resolution. For achieving narrow bandwidth, triple FPI was proposed earlier by Ramsay et.al [13]. In another excellent work computer is used to control the three reference interferometers which establish the spacing of the three FPIs [14].

To avoid the transmission losses usually encountered in a tandem arrangement of several two mirror FPIs, multi-mirror FPI concept was proposed. Another advantage associated with multi-mirror FPI is the shape of the transmission pass band which can become more nearly rectangular and provide better side lobe suppression [15].

The frequency range between two adjacent transmitted peaks and the Full Width Half Maximum (FWHM) of a FPI can be independently controlled. The cavity gap sets the Free Spectral Range (FSR) and the mirrors reflectivity controls the Full Width Half Maximum (FWHM). The transmission peaks can be made very sharp by increasing the reflectivity of the mirror surfaces.

Recent developments in micromachining and etching techniques make multi-mirror FPI based MEMS sensor feasible. In this paper a new MEMS based optical four-mirror tunable FPI having spectral range in IR region is proposed. Also a simple model of the MEMS four-mirror FPI is proposed. The main aim of this four-mirror FPI is to increase spectral range of operation in infrared region having applications in many areas such as forensic science and in metabolic fingerprinting using the IR spectrum (2500-7000 nm) [15].

## 2. Theory

Matrix method was suggested by the analysis of multilayer thin films [16-18]. Suppose that  $N$  partially transmitting plane parallel mirrors of negligible thickness is sequentially numbered  $i=1, 2, \dots, N$ . In Figure 1  $E_i^+$  is the amplitude of the electric field vector on the left hand side of  $i^{\text{th}}$  mirror for a wave front propagating to the right,  $E_i^-$  is the amplitude on the left hand side of the  $i^{\text{th}}$  mirror for a wave front traveling to the left.  $r_i$  and  $t_i$  are the amplitude reflection and transmission coefficient for  $i^{\text{th}}$  mirror. The distance from  $i^{\text{th}}$  mirror to  $(i+1)^{\text{th}}$  mirror is  $L_i$ . In terms of phase length  $\Phi_i$ ,  $L_i$  can be written as:

$$\Phi_i = 2\pi L_i / \lambda \quad (1)$$

For series of  $N$  parallel, partially transmitting mirrors the general result is:

$$\begin{bmatrix} E_{1^+} \\ E_{1^-} \end{bmatrix} = (1/t_1 t_2 \dots t_{N-1}) \begin{bmatrix} \exp^{-i\Phi_1} & -r_1 \exp^{i\Phi_1} \\ -r_1 \exp^{-i\Phi_1} & \exp^{i\Phi_1} \end{bmatrix} \dots \begin{bmatrix} \exp^{-i\Phi_{N-1}} & -r_{N-1} \exp^{i\Phi_{N-1}} \\ -r_{N-1} \exp^{-i\Phi_{N-1}} & \exp^{i\Phi_{N-1}} \end{bmatrix} \begin{bmatrix} E_{N^+} \\ E_{N^-} \end{bmatrix}$$

$$\begin{bmatrix} E_{1^+} \\ E_{1^-} \end{bmatrix} = (1/t_1 t_2 \dots t_{N-1}) \begin{bmatrix} A & B \\ C & D \end{bmatrix} \begin{bmatrix} E_{N^+} \\ E_{N^-} \end{bmatrix} \tag{2}$$

Where  $A$ ,  $B$ ,  $C$  and  $D$  are the coefficients of the resulting matrix.

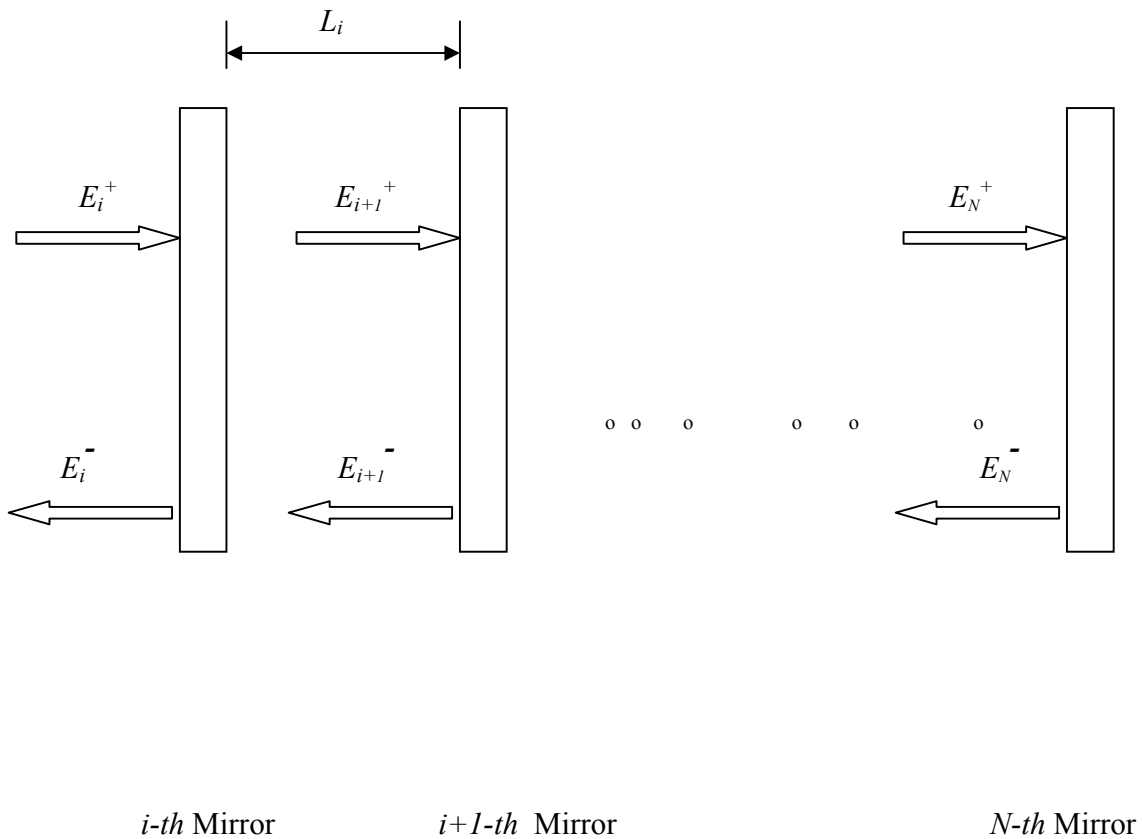


**Figure 1.** The amplitudes transmission and reflection at  $i^{th}$  mirror,  $(i + 1)^{th}$  up to  $N$  mirrors.

The amplitude of the transmission ( $a_t$ ) of such a stack of  $N$  mirrors is schematically shown in Figure 1

Where,  $a_t = t_N E_N^+ / E_1^+$

$$a_t = (t_1 t_2 \dots t_N) E_N^+ / (A E_N^+ + B E_N^-)$$

or  $a_t = t_1 t_2 \dots t_N / (A - r_N B)$ . (3)

For four mirrors FPI, put  $N=4$  in the above mentioned equation (2), the amplitude of the transmission is:

$$\begin{bmatrix} E_{1+} \\ E_{1-} \end{bmatrix} = (1/t_1 t_2 t_3) \begin{bmatrix} \exp^{-i\Phi_1} & -r_1 \exp^{i\Phi_1} \\ -r_1 \exp^{-i\Phi_1} & \exp^{i\Phi_1} \end{bmatrix} \begin{bmatrix} \exp^{-i\Phi_2} & -r_2 \exp^{i\Phi_2} \\ -r_2 \exp^{-i\Phi_2} & \exp^{i\Phi_2} \end{bmatrix} \begin{bmatrix} \exp^{-i\Phi_3} & -r_3 \exp^{i\Phi_3} \\ -r_3 \exp^{-i\Phi_3} & \exp^{i\Phi_3} \end{bmatrix} \begin{bmatrix} E_{4+} \\ E_{4-} \end{bmatrix}$$

On simplification the above equation can be rewritten as:

$$\begin{bmatrix} E_{1+} \\ E_{1-} \end{bmatrix} = (1/t_1 t_2 t_3) \begin{bmatrix} A & B \\ C & D \end{bmatrix} \begin{bmatrix} E_{4+} \\ E_{4-} \end{bmatrix} \quad (4)$$

Where

$$A = \exp^{-i(\theta_1 + \theta_2 + \theta_3)} + r_1 r_2 \exp^{i(\theta_1 - \theta_2 - \theta_3)} + r_2 r_3 \exp^{-i(\theta_1 - \theta_2 + \theta_3)} + r_1 r_3 \exp^{i(\theta_1 + \theta_2 - \theta_3)} \quad (5)$$

$$B = -r_1 \exp^{i(\theta_1 + \theta_2 + \theta_3)} - r_2 \exp^{-i(\theta_1 - \theta_2 - \theta_3)} - r_3 \exp^{-i(\theta_1 + \theta_2 - \theta_3)} - r_1 r_2 r_3 \exp^{i(\theta_1 - \theta_2 + \theta_3)} \quad (6)$$

$$C = -r_1 \exp^{-i(\theta_1 + \theta_2 + \theta_3)} - r_2 \exp^{i(\theta_1 - \theta_2 - \theta_3)} - r_3 \exp^{i(\theta_1 + \theta_2 - \theta_3)} - r_1 r_2 r_3 \exp^{-i(\theta_1 - \theta_2 + \theta_3)} \quad (7)$$

$$D = r_1 r_3 \exp^{-i(\theta_1 + \theta_2 - \theta_3)} + r_2 r_3 \exp^{i(\theta_1 - \theta_2 + \theta_3)} + r_1 r_2 \exp^{-i(\theta_1 - \theta_2 - \theta_3)} + \exp^{i(\theta_1 + \theta_2 + \theta_3)} \quad (8)$$

The amplitude transmission ( $a_t$ ) of such a stack of four-mirror is

$$a_t = (t_1 t_2 t_3 t_4) / (A - r_4 B)$$

The intensity transmission ( $T$ ) is given by:

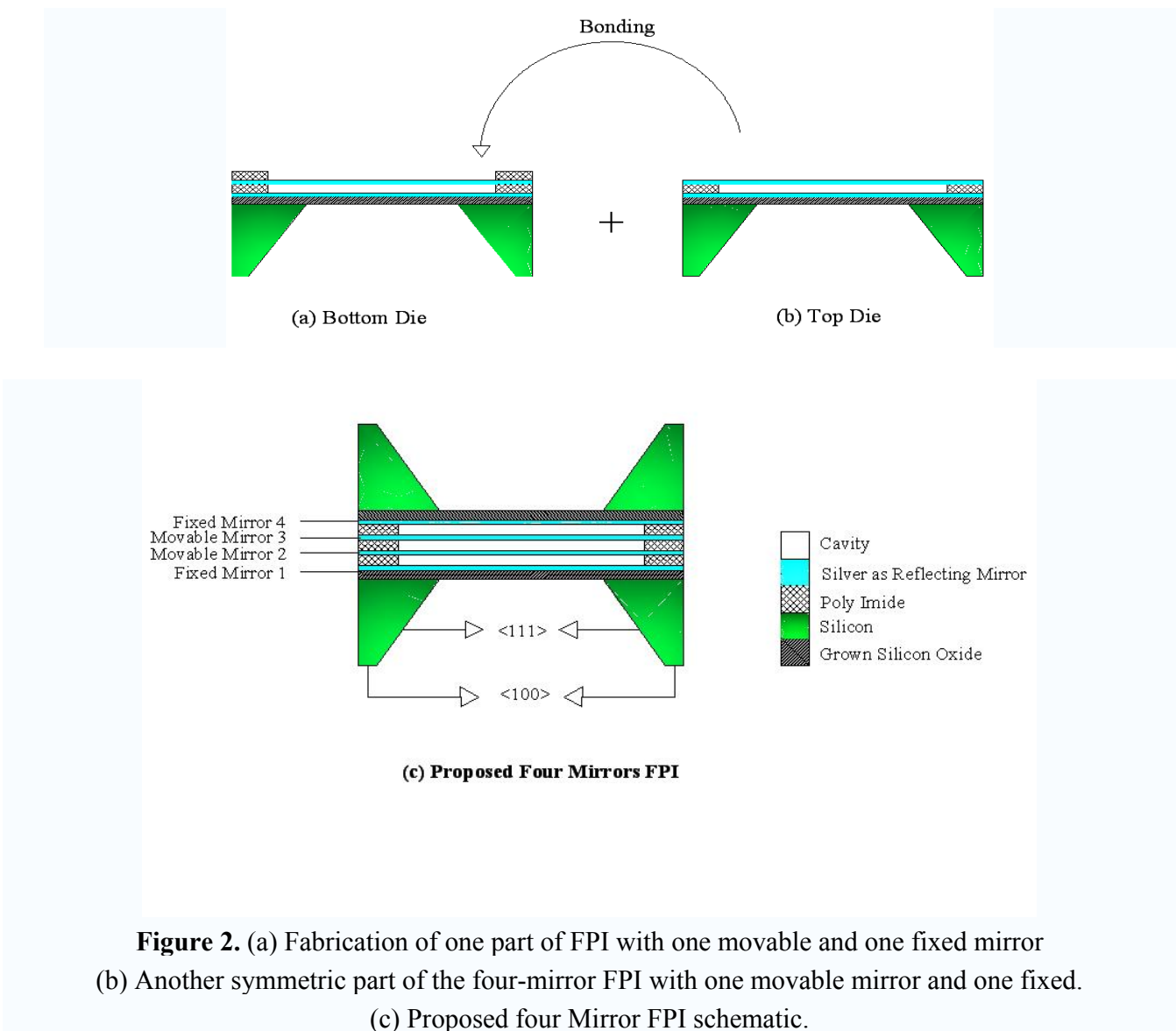
$$T = a_t a_t^*$$

Where  $a_t^*$  is the conjugate of  $a_t$ .

$$T = t_1 t_2 t_3 t_4 / (\exp^{[i(-\theta_1 - \theta_2 - \theta_3)]} + r_1 r_2 \exp^{[i(\theta_1 - \theta_2 - \theta_3)]} + r_2 r_3 \exp^{[i(-\theta_1 + \theta_2 - \theta_3)]} + r_1 r_3 \exp^{[i(\theta_1 + \theta_2 - \theta_3)]} + r_3 r_4 \exp^{[i(-\theta_1 - \theta_2 + \theta_3)]} + r_1 r_2 r_3 r_4 \exp^{[i(\theta_1 - \theta_2 + \theta_3)]} + r_2 r_4 \exp^{[i(-\theta_1 + \theta_2 + \theta_3)]} + r_1 r_4 \exp^{[i(\theta_1 + \theta_2 + \theta_3)]}). \quad (9)$$

Where  $\theta_1$ ,  $\theta_2$  and  $\theta_3$  are phase cavity lengths of the three cavities respectively which can be calculated using equation (1).

### 3. Proposed Fabrication Method



Proposed four mirrors tunable FPI is symmetrical in the design. Silver was selected as the mirror material due to its high reflectivity in IR range. Fabrication process starts with the growing of oxide on the silicon followed by anisotropic wet etching from the back side of the (100) silicon wafer in KOH or TMAH (Tetra Methyl Ammonium Hydroxide) till the grown oxide layer is reached. Silver is deposited on oxide layer followed by the deposition of polyamide. Polyamide layer is sacrificially etched with silver on both of its side. Three cavities of the proposed FPI were formed by the sacrificial etching of the polyamide. Same process can be used for fabricating the similar die again having a movable mirror and a fixed mirror as shown in Figure 2a and Figure 2b, and join the two symmetrical dies with patterned polyimide layer in between them with any bonding method. The final design is shown in Figure 2c.

## 4. Analysis

### 4.1 Fixing of the cavity length:

The mirrors or the reflecting surfaces should be optically flat. Flatness affects the spectral width and radiation passing through the filter. Reflectivity of the surfaces were selected as  $r_1=r_4=0.8366$  and  $r_2=r_3=0.99$  [15]. In the un-tuned state the spectral response for different cavity lengths of 600nm, 700nm and 800nm were recorded Figure 3. For this paper, 600nm was selected as cavity length.

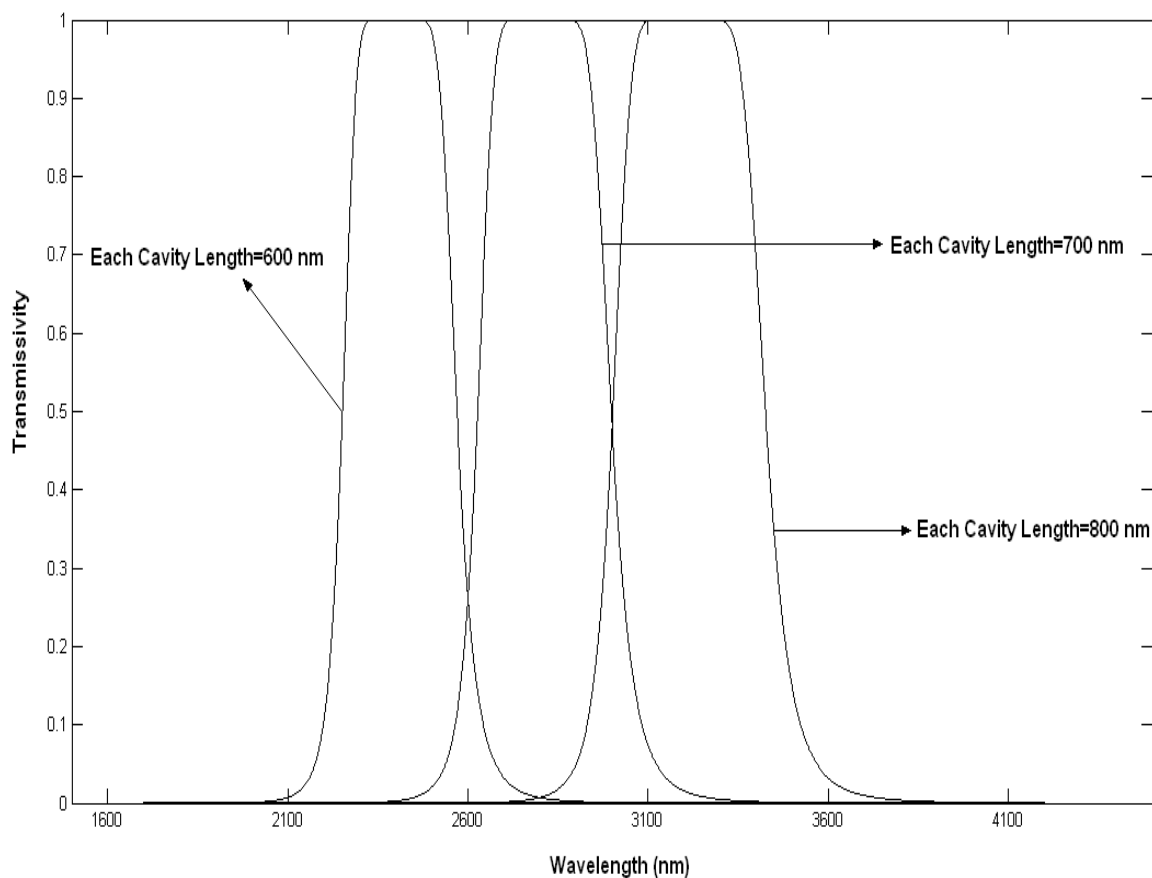


**Figure 3.** Spectral response of three cavity FPI with different cavity lengths of 600nm, 700nm and 800nm.

Two different cases were considered, one in which the tuning is achieved by deflecting one of the middle mirror and other in which both the middle mirrors were deflected for the tuning of the four-mirror FPI. Change in the spectral response was recorded for both cases.

#### 4.2 Case One: (Only one mirror deflection)

In first case, one of the two middle mirrors (either the second or the third) was electrostatically deflected, and the corresponding spectral response is plotted for each tuned position. If  $\Delta_1$  and  $\Delta_2$  are the deflections for mirror 2 and 3, then cavity lengths will change as given in equation (10), (11) and (12) for each tuned position.

Then cavity lengths become,

$$L_1 = L_1 - \Delta_1; \quad (10)$$

$$L_2 = L_2 + \Delta_1 + \Delta_2; \quad (11)$$

$$L_3 = L_3 - \Delta_2; \quad (12)$$

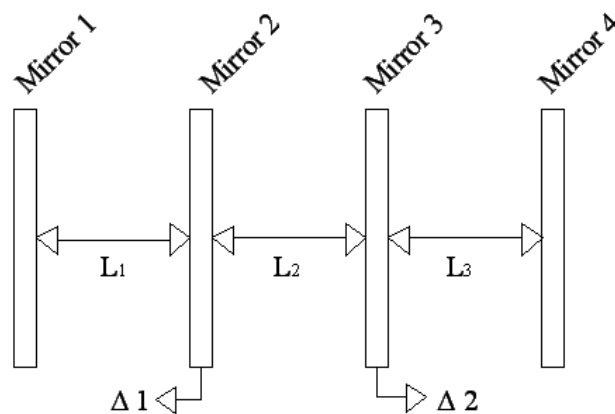


**Figure 4.** Schematic Diagram of four-Mirror FPI.

In the Figure 4  $L_1$ ,  $L_2$  and  $L_3$  are the three cavity lengths. Mirror 1 and mirror 4 are fixed mirrors whereas mirrors 2 and 3 are movable ones having deflections  $\Delta_1$  and  $\Delta_2$  respectively in the indicated directions for tuning the FPI for different wavelength in IR spectrum.

##### 4.2.1 Spectral response in case one: (Only one mirror deflection $\Delta_2=0$ )

In the first case  $\Delta_2$  is zero as mirror 2 is fixed (not active) the FPI is tuned with only one mirror. From the spectral response plotted in Figure 5 for each 20nm deflection of the mirror 2 it is evident that the transmissivity of FPI is around 80% in most of the tuned positions and the possible tuned wavelength ranges from 2400nm to 3400nm approximately. One advantage of the four mirrors FPI is the decrease in bandwidth with the tuning. The angular separation of principal peaks observed in the first two or three subplots clearly reveals the increase in the field spectral range in the multi cavity FPI. As in the proposed four-mirror FPI cavity lengths were initially fixed at 600nm so we could not deflect the mirror 2 more than 200nm as keeping the snap voltage in mind [19]. Snap Voltage is a limiting value beyond which the reflecting mirrors become unstable and snaps onto the back plate.

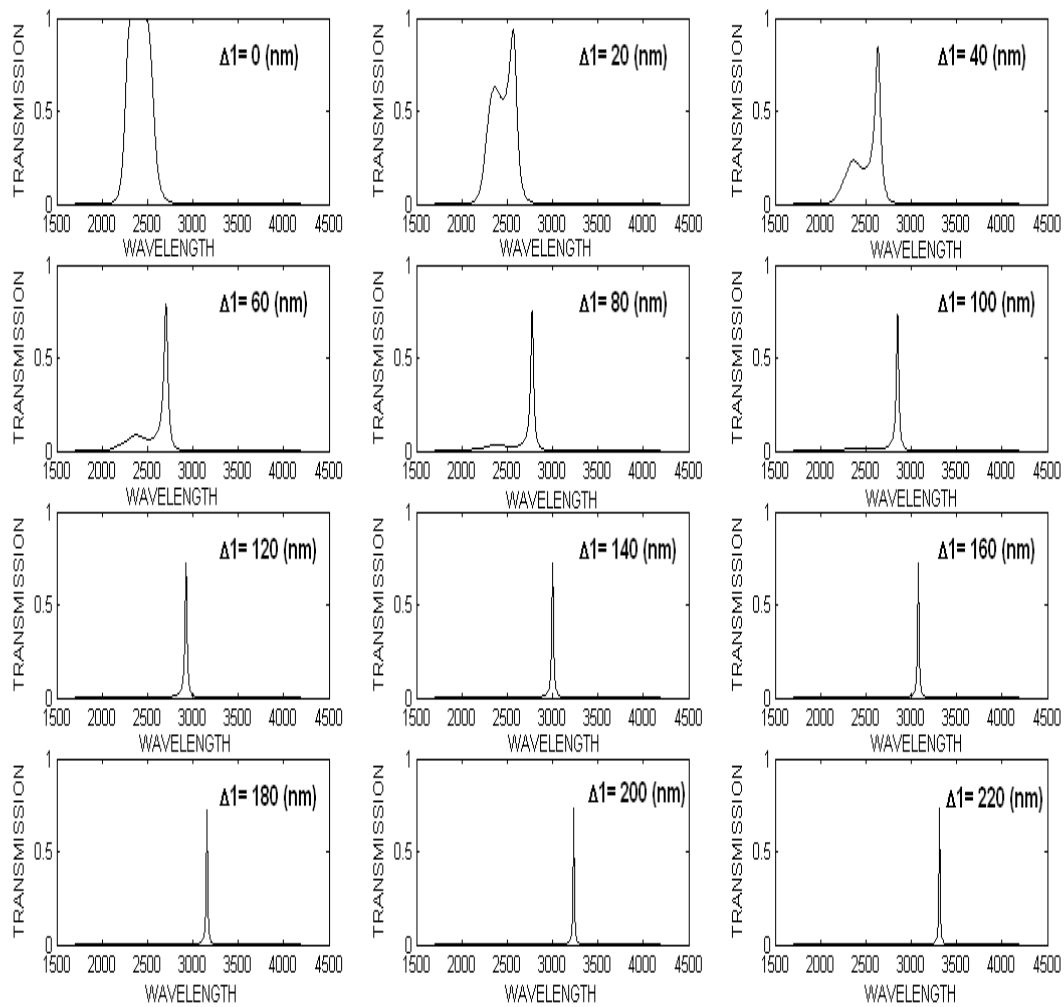


**Figure 5.** Spectral response of FPI when tuned by deflecting mirror 2 by  $\Delta_1$  and keeping  $\Delta_2$  at zero for all the responses .

#### 4.3 Case Two: (Both middle mirrors 2 & 3 deflected with equal amount)

##### 4.3.1 Two middle mirrors were deflected simultaneously for equally deflection ( $\Delta_1 = \Delta_2$ )

If mirror 2 is deflected by  $\Delta_1$  and mirror 3 is deflected simultaneously with  $\Delta_2$  then the three cavity lengths were changed accordingly as given in equation (10), (11) and (12). Both the middle mirrors 2 & 3 were deflected simultaneously with equal deflections for every tuned position and the spectral response for each tuned position is plotted in Figure 6.

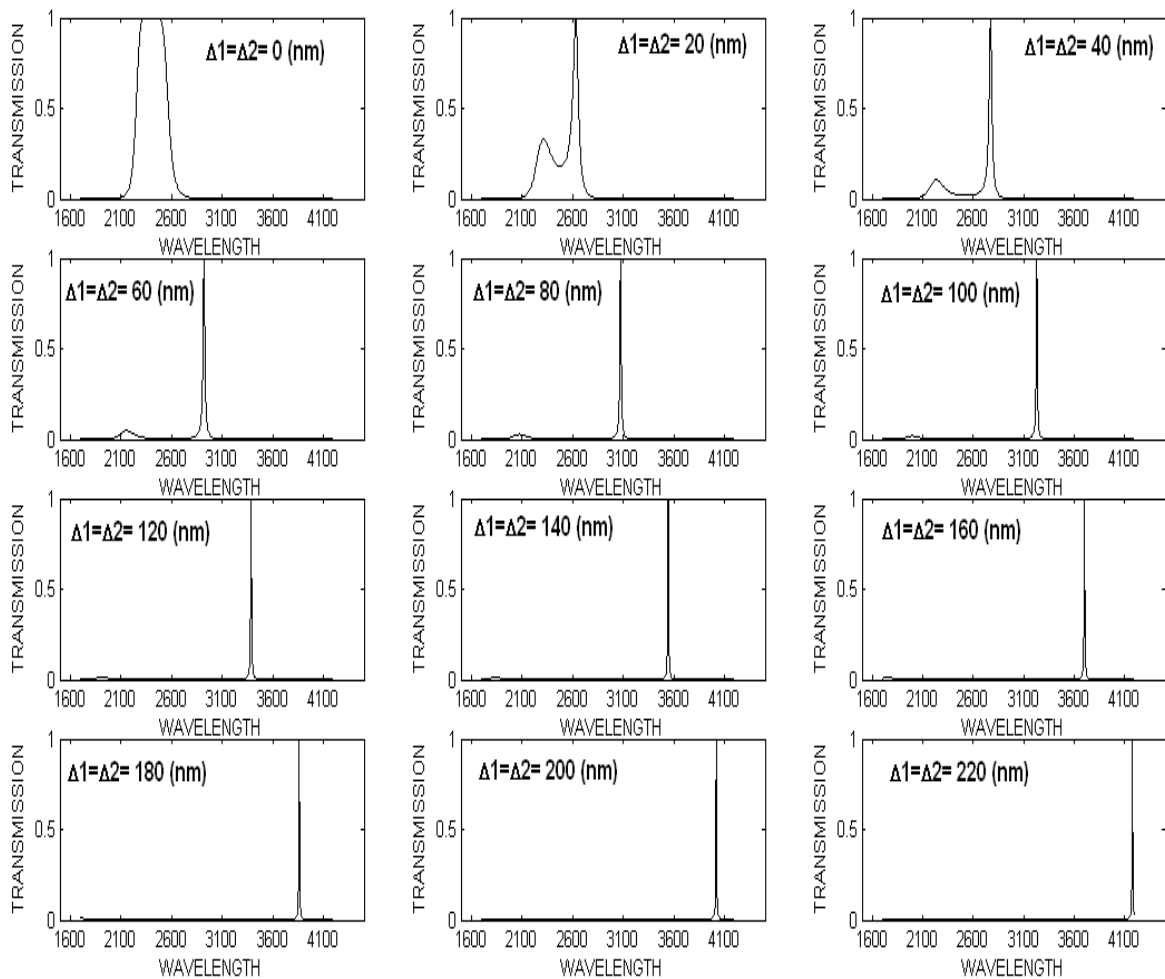


**Figure 6.** Spectral response of FPI when tuned by deflecting two middle mirrors 2 and 3 by equal deflection  $\Delta_1 = \Delta_2$  for each tuned position.

#### 4.3.2 Spectral response in case two: ( $\Delta_1 = \Delta_2 \neq 0$ )

From the spectral response plotted in Figure 6 for each 20nm deflection of the two mirrors it is evident that the transmissivity of FPI is above 90% in most of the tuned positions and the tuned wavelength ranges from 2500nm to 4100nm approximately; from the spectral response plotted in Figure 5 and Figure 6, it is evident that the tunability increases in case two when tuning was achieved by deflecting the middle mirrors 2 and 3. High tuning efficiency and high spectral range with decrease in band width can be achieved when mirrors 2 and 3 were deflected independently for each tuned positions.

#### 4.3.3 Maximum Tuned wavelength for each deflection

Smooth tunability of three cavity FPI can be achieved by deflecting the two middle mirrors independently for each tuned wavelength as shown the Figure 7.

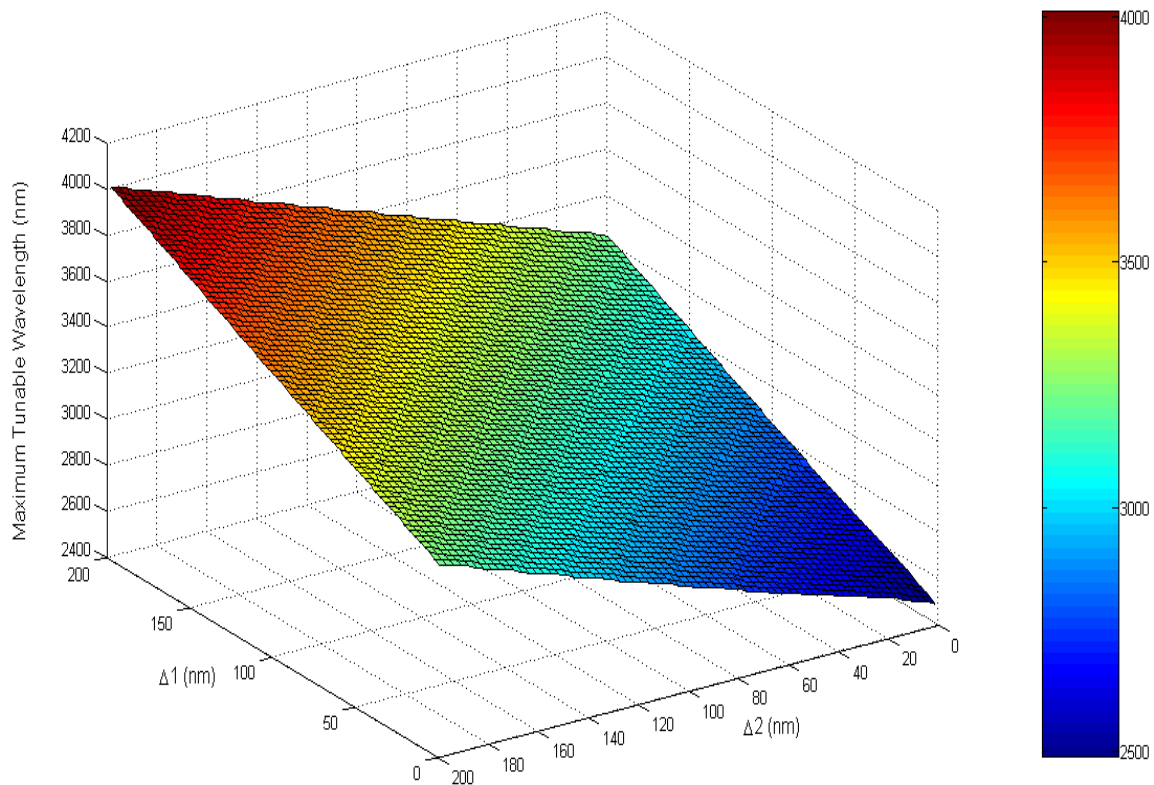


**Figure 7.** Tuned wavelength in nanometer is plotted corresponding to each independent deflection  $\Delta_1$  and  $\Delta_2$  in mirrors 2 and 3 respectively.

It is evident from the axionometric three dimensional plot in Figure 7 that the spectral range varies from 2400nm to 4018nm with the possible deflections of  $\Delta_1$  and  $\Delta_2$  respectively. The transition from lower wavelength to higher wavelength is achieved smoothly with a sensitivity of 5.3nm (slope of the curve) for every nanometer deflection in either of the two middle mirrors.

#### 4.3.4 Full Width Half Maximum (FWHM)

FWHM is plotted in Figure 8 with respective deflections ( $\Delta_1$  and  $\Delta_2$ ) in the middle mirrors. FWHM changes with the tuning of the FPI. FWHM decreases with the increase in the corresponding deflections of the middle mirrors. FWHM varies from 120nm to less than 10nm if, tuning is achieved by varying  $\Delta_1$

from (0 -200) nm and  $\Delta_2$  from (30 to 100) nm. The FWHM is approximately, below 20nm for most of the tuned spectral range of the FPI. One of the advantages of four mirror FPI is its low FWHM in most of the tuned positions.

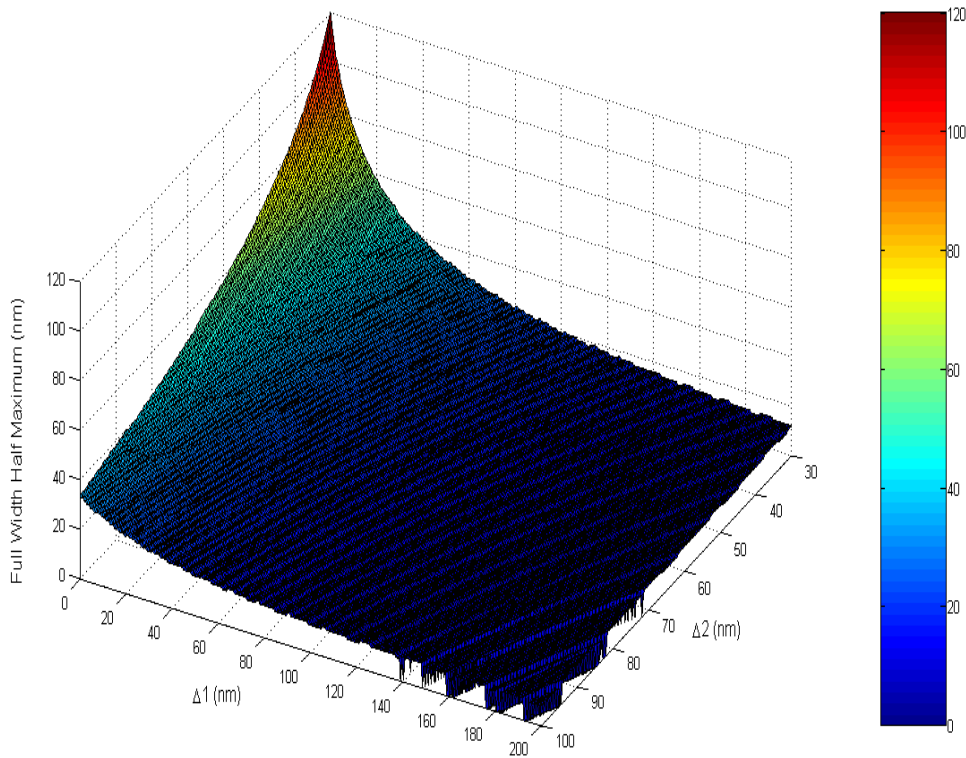


**Figure 8.** FWHM is plotted for each tuned wavelength corresponding to independent deflections in two middle mirrors.

## 5. Conclusion

In four mirror MEMS based FPI the tuning is achieved either by moving one or both middle mirrors. Performance of the FPI is better in terms of spectral range and percentage transmission, when the tuning is achieved by deflecting both middle mirrors in comparison to the performance when single mirror is used for the tuning of the FPI. The spectral range achieved is 2400-4018 nm when tuned with both the middle mirrors and the sensitivity of the FPI is 5.3nm for every nm deflection in either of the two middle mirrors. FWHM is below 20nm for most of the tuned positions. The proposed three cavity tunable MEMS Fabry Perot Interferometer will be fabricated in the near future for validation of the model.

## References

1. Onat, B. M.; Masaun, N.; Huang, W.; Lange, M.; Dries, C. Hyperspectral Imaging with MEMs integrated focal plane arrays. *Semiconductor Photodetectors II* **2005**, 5726, 92–102.
2. Carrano, J.; Brown, J.; Perconti, P.; Barnard, K. Tuning into detection. *SPIE Oemagazine* **2004**, 20–22.
3. Saari, H.; Mannila, R.; Antila, J.; Blomberg, M.; Rusanen, O.; Tenhunen, J.; Wolf, L.; Harnisch, B. Miniaturised gas sensor using a micromachined Fabry–Pérot interferometer. *Preparing for the Future* **2000**, 10, 4–5.
4. Kotidis, P.; Atia, W.; Kuznetsov, M.; Fawcett, S.; Nislick, D.; Crocombe, R.; Flanders, D. C. Optical tunable filter-based micro-instrumentation for industrial applications. *Proc. Instr. Syst. and Autom. Soc. (ISA)* **2003**, 1–14.
5. Keating, A. J.; Silva, K. K.; Dell, J. M.; Musca, C. A.; Faraone, L. Optical Characterization of Fabry-Pérot MEMS Filters Integrated on Tunable Short-Wave IR Detectors. *IEEE Photon. Tech. Lett.* **2006**, 18, 1079-1081.
6. Hohlfeld, D.; Epmeier, M.; Zappe, H. A thermally tunable Silicon based optical filter. *Sensors Actuators A* **2003**, 103, 93-99.
7. Aziz, M.; Pfeiffer, J.; Wohlfarth, M.; Lubber, C.; Wu, S.; Meissner, P. A new and simple concept of tunable two-chip microcavities for filter applications in WDM systems. *IEEE Photon. Tech. Lett.* **2000**, 12, 1522-1524.
8. Yun, S.S.; Lee, J.H. A micromachined in plane tunable optical filter using the thermo-optic effect of crystalline silicon. *Micromech. Microeng* **2003**, 721-725.
9. Meisner, P.; Aziz, M.; Halbritter, H.; Riemenschneider, F.; Pfeiffer, J.; Hermes, T. Micromachined two-chip WDM filters with stable half symmetric cavity and their system integration. *Electronic Components and Technology Conference* **2002**, 52, 34-41.
10. Loughhead, R. E.; Bray, R. J.; Brown, N. Instrumental profile of a triple Fabry-Perot interferometer for use in solar spectroscopy. *Appl. Opt.* **1978**, 17, 415-419.
11. Roesler, F. L. In *Methods of Experimental Physics*; Marton, L., Ed.; Academic Press: New York, **1974**; Volume 12A, pp. 540-541.
12. Roychoudhuri, C.; Hercher, M. Stable multipass Fabry-Perotinterferometer: design and analysis. *Appl. Opt.* **1977**, 16, 2514-2520.
13. Ramsay, J. V.; Kobler, H.; Mugridge, E. G. V. A new tunable filter with a very narrow pass band. *Solar Phys.* **1970**, 12, 492-501.
14. Bray, R. J. Computer controlled narrow band optical filters in solar astronomy. *Radiopyysics and Quantum Electronics* **1977**, 20, 1318-1330.
15. Ellis, D. I.; Goodacre, R. Metabolic fingerprinting in disease diagnosis: biomedical applications of infrared and Raman spectroscopy. *Analyst* **2006**, 131, 875-885.

16. van de Stadt, H.; Muller, J. M. Multimirror Fabry Perot Interferometer. *Opt. Soc. Am. A* **1985**, *2*, 1363-1370.
17. MacLeod, H. A. *Thin Film Optical Filters*; Hilger: London, U.K., 1969; pp. 303-320.
18. Born, M.; Wolf, E. *Principles of Optics*; Pergamon: Oxford, U.K., 1970; pp. 366-368.
19. Packirisamy, M. Microfabrication Influence on the Behavior of Capacitive Type MEMS Sensors and Actuators. *Sensor Review* **2006**, *26*, 58-65.
- 20.

© 2007 by MDPI (<http://www.mdpi.org>). Reproduction is permitted for noncommercial purposes.